PERGAMON

Chemical Engineering Science 54 (1999) 1751–1757

Chemical Engineering Science

Influence of isotherm inflection on diffusion in silicalite

R. Krishna*, T.J.H. Vlugt, B. Smit

Department of Chemical Engineering, University of Amsterdam, Nieuwe Achtergracht 166, 1018 WV Amsterdam, The Netherlands

Received 27 August 1998; accepted 11 December 1998

Abstract

Adsorption isotherms of benzene, *p*-xylene, *n*-hexane, *n*-heptane and branched alkanes in silicalite show inflection behaviour; this behaviour is adequately modelled using a dual-site Langmuir model. In this model we make a distinction between two sites with different sorption characteristics: (1) site A which refer to the intersections between the straight channels and the zig-zag channels, and site B which refers to the channel interiors (straight or zig-zag channels). Using the Maxwell–Stefan theory of diffusion in zeolites, the influence of the isotherm inflection on the Fick diffusivity of pure components in silicalite is shown to be characterized by two extrema. For a mixture of *n*-hexane and 3-methyl pentane, the dual-site Langmuir model for the mixture predicts a curious maximum in the loading of the branched alkane; this mixture behaviour is confirmed by Configurational-Bias Monte Carlo simulations. The Maxwell–Stefan theory is used to demonstrate the possibility of separating the hydrocarbon isomers by permeation across a silicalite membrane.

Keywords: Zeolite diffusion; Dual-site Langmuir isotherm; Configurational bias Monte Carlo techniques; Fick diffusivity; Maxwell–Stefan theory; Thermodynamic correction factor

1. Introduction

For adsorption of benzene, *p*-xylene, *n*-hexane and *iso* butane on silicalite several experimental studies have shown that the isotherm exhibits inflection behaviour (Guo et al., 1989; Sun et al., 1996, 1998; Takaishi et al., 1998; Song and Rees, 1997). The inflection in the isotherm is due to the preferential location of molecules at certain sites in the silicalite structure. Broadly speaking, we can identify two distinct adsorption sites: (1) Site A, which represents the intersections between the straight channels and the zig-zag channels, and (2) Site B, which represents the channel interiors; see Fig. 1. Using Configurational-bias Monte Carlo (CBMC) simulation techniques, Vlugt et al. (1998) have shown that the inflection behaviour for 2-methyl alkanes (with 4,5,6 and 7 C atoms) is caused because these molecules prefer to occupy the intersections (Site A). However, at a loading, θ, of 4 molecules per unit cell (corresponding to 0.6935 mmol/g of silicalite) the intersections are all fully occupied. To obtain loadings higher than 4, these branched molecules must seek residence in the channel interiors, which is energetically more demanding. This leads to an inflection in the isotherm.

The dual-site Langmuir (DSL) model

$$\theta = \frac{\theta_A k_A p}{1 + k_A p} + \frac{\theta_B k_B p}{1 + k_B p} = \frac{(\theta_A k_A + \theta_B k_B)p + (\theta_A + \theta_B)k_A k_B p^2}{1 + (k_A + k_B)p + k_A k_B p^2} \quad (1)$$

has been used to describe the isotherm for *n*-hexane (Micke et al., 1994; Song and Rees, 1997). As can be seen from Fig. 2, the DSL model provides a very good representation of the isotherms of benzene and *n*-hexane. Vlugt et al. (1999) have shown that the DSL model provides an excellent representation of the CBMC simulations of sorption isotherms of linear alkanes (with 6–8 C atoms) and branched alkanes (with C atoms ranging from 4 to 7); in all cases the inflection is observed at a loading of 4 molecules per unit cell and so $\theta_A = 4$.

* Corresponding author. Tel.: +31 20 525 7007; fax +31 20 525 5604; e-mail: krishna@chemeng.chem.uva.nl.

0009-2509/99/$ – see front matter
PII: S0009-2509(98)00538-7

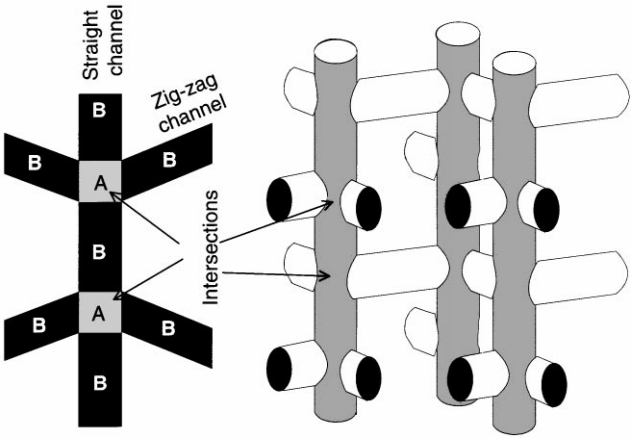

Fig. 1. Sorption sites within silicalite.

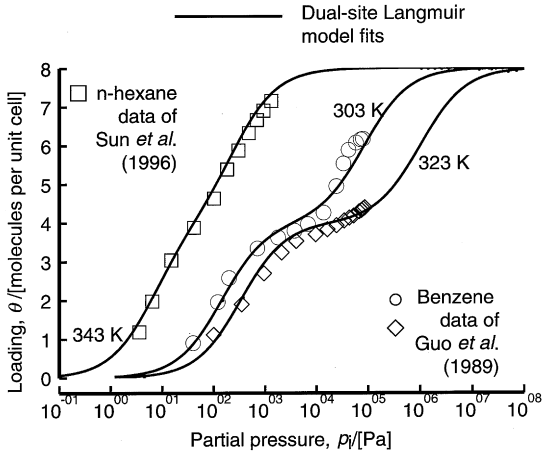

Fig. 2. Pure component isotherms for sorption in silicalite-1. (a) Experimental data of Sun et al. (1996). for *n*-hexane at 343 K; the DSL model fit parameters are: $\theta_{1A} = 4$, $\theta_{1B} = 4$, $k_{1A} = 0.15\ \mathrm{Pa}^{-1}$, $k_{1B} = 4 \times 10^{-3}\ \mathrm{Pa}^{-1}$. (b) Experimental data for benzene at 303 K from Guo et al. (1989); the DSL model fit parameters are: $\theta_{1A} = 4$, $\theta_{1B} = 4$, $k_{1A} = 7 \times 10^{-3}\ \mathrm{Pa}^{-1}$, $k_{1B} = 1.2 \times 10^{-5}\ \mathrm{Pa}^{-1}$. (c) Experimental data for benzene at 323 K from Guo et al. (1989); the DSL model fit parameters are: $\theta_{1A} = 4$, $\theta_{1B} = 4$, $k_{1A} = 3 \times 10^{-3}\ \mathrm{Pa}^{-1}$, $k_{1B} = 1 \times 10^{-6}\ \mathrm{Pa}^{-1}$.

The objectives of the present communication are three-fold:

(1) to derive the consequences of the isotherm inflection on the diffusion behaviour of pure components in silicalite,
(2) to examine the sorption and diffusion characteristics of mixtures, each component of which exhibits inflection behaviour, and
(3) to demonstrate the possibility of separation of isomers of linear and branched alkanes by permeation through a silicalite membrane.

In order to describe the influence of sorption on diffusion we make use of the Maxwell–Stefan theory for diffusion in zeolites described in our earlier work (Krishna, 1990, 1993a,b; Krishna and Wesselingh, 1997).

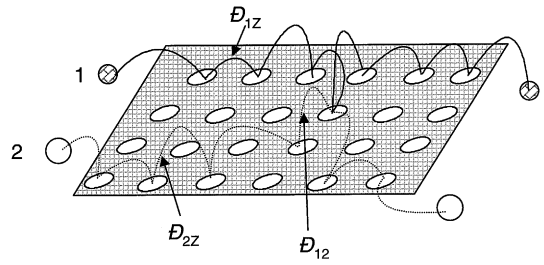

Fig. 3. Pictorial representation of the Maxwell–Stefan diffusivities.

2. The Maxwell–Stefan theory for zeolite diffusion

Using the Maxwell–Stefan theory for microporous diffusion the following expression can be derived for diffusion of species i in a zeolite (Krishna, 1993a,b):

$$-\frac{1}{RT}\frac{\mathrm{d}\mu_i}{\mathrm{d}z} = \sum_{\substack{j=1 \\ j\neq i}}^{n} \frac{\theta_j}{\theta_{\max}} \frac{u_i - u_j}{Đ_{ij}} + \frac{u_i}{Đ_{iZ}};\ i = 1, 2, \ldots, n, \qquad (2)$$

where $-\mathrm{d}\mu_i/\mathrm{d}z$, the chemical potential gradient, is the force acting on species i tending to move it within the zeolite at a velocity u_i, $Đ_{iZ}$ is the Maxwell–Stefan diffusivity describing the interaction between component i and the zeolite (Z), and $Đ_{ij}$ is the Maxwell–Stefan describing the interchange between components i and j within the zeolite structure. The $Đ_{iZ}$ are also called the corrected diffusivity in the literature; cf. Ruthven (1984). Fig. 3 is a pictorial representations of the three Maxwell–Stefan diffusivities describing diffusion of a binary mixture consisting of species 1 and 2. Procedures for estimation of the $Đ_{iZ}$ and the interchange diffusivity $Đ_{ij}$ are discussed by Krishna (1993a,b). If there is no possibility of interchange between species 1 and 2 as in single file diffusion, the first term on the right side of Eq. (2) can be ignored. Writing Eq. (2) in terms of the diffusion fluxes N_i

$$N_i \equiv \rho\theta_i u_i \qquad (3)$$

we get

$$-\frac{\theta_i}{RT}\frac{\mathrm{d}\mu_i}{\mathrm{d}z} = \sum_{j=1}^{n} \frac{\theta_j N_i - \theta_j N_j}{\rho\theta_{\max} Đ_{ij}} + \frac{N_i}{\rho Đ_{iZ}},\ i = 1, 2, \ldots, n, \qquad (4)$$

where θ_i is the molecular loading within the zeolite, expressed in molecules per unit cell, $\theta_{\max}$ is the maximum molecular loading, $\theta_{\max} = (\theta_A + \theta_B)$, and ρ represents the number of unit cells per m^3 of silicalite.

The chemical potential gradients are related to the gradients in the component loadings by

$$\frac{\theta_i}{RT}\frac{\mathrm{d}\mu_i}{\mathrm{d}z} = \sum_{j=1}^{n} \Gamma_{ij}\frac{\mathrm{d}\theta_j}{\mathrm{d}z},\ \Gamma_{ij} \equiv \frac{\theta_i}{p_i}\frac{\partial p_i}{\partial \theta_j},\ i, j = 1, \ldots, n, \qquad (5)$$

where we have defined a matrix of thermodynamic correction factors $[\Gamma]$. The elements Γ_{ij} of this matrix can be determined from a knowledge of the sorption isotherms. Combining Eqs. (2)–(5) we can write down an explicit expression for the fluxes N_i using n-dimensional matrix notation

$$(N) = -\rho[B]^{-1}\,[\Gamma]\,\frac{\mathrm{d}(\theta)}{\mathrm{d}z}, \tag{6}$$

where the elements of the matrix $[B]$ are

$$B_{ii} = \frac{1}{Đ_{iZ}} + \sum_{\substack{j=1\\ j\neq i}}^{n} \frac{\theta_j}{Đ_{ij}},\ B_{ij} = -\frac{\theta_i}{Đ_{ij}},\ i, j = 1, 2, \ldots, n. \tag{7}$$

The more commonly used Fick diffusivity matrix is defined as

$$(N) = -\rho[D]\,\frac{\mathrm{d}(\theta)}{\mathrm{d}z}. \tag{8}$$

Comparing Eqs. (5) and (6) we obtain the following inter-relation between the Fick and the Maxwell–Stefan diffusivities

$$[D] = [B]^{-1}[\Gamma]. \tag{9}$$

Since the thermodynamic correction factor matrix $[\Gamma]$ is generally non-diagonal, the matrix of Fick diffusivities is also generally non-diagonal. Generally speaking the M-S diffusivities $Đ_{iZ}$ are better behaved than the elements of Fick diffusivity matrix $[D]$. The latter diffusivities are strongly influenced by the thermodynamic non-idealities in the system. In this paper we examine, in turn, the influence of $[\Gamma]$ on the diffusion behaviour of single components and binary mixtures in silicalite for which the isotherms are described by the dual-site Langmuir model.

3. Diffusion of a single component in silicalite

For single component diffusion Eqs. (4) and (7) degenerate to their scalar forms

$$\Gamma = \frac{\theta}{p}\frac{\partial p}{\partial \theta} \tag{8}$$

and

$$D = Đ\Gamma. \tag{9}$$

For the DSL model isotherm, the thermodynamic factor can be determined by analytic differentiation of Eq. (1); the result is

$$\Gamma = \left[\begin{array}{c} \dfrac{[1+(k_A+k_B)p+k_Ak_Bp^2]^2}{[1+(k_A+k_B)p+k_Ak_Bp^2][(\theta_Ak_A+\theta_Bk_B)+\theta_{\max}2k_Ak_Bp]} \\ -[(\theta_Ak_A+\theta_Bk_B)p+\theta_{\max}k_Ak_Bp^2][(k_A+k_B)+2k_Ak_Bp]. \end{array}\right]\frac{\theta}{p} \tag{10}$$

This correction factor shows two extrema: a maximum at the inflection point $\theta_A = 4$ and a minimum at a loading $\theta_A < \theta < \theta_B$. This behaviour is illustrated for adsorption of benzene on silicalite at temperatures of 303 and 323 K; see Figs. 4 (a) and (b). Since the Fick diffusivity is proportional to the thermodynamic factor, it can be expected to also exhibit two extrema. This is indeed verified by the experimental data of Shah et al. (1995) for Fick diffusivity at 303 and 323 K; see Figs. 4(c) and (d). The Maxwell–Stefan diffusivities, calculated from $Đ = D/\Gamma$, are seen to be practically constant, emphasising the importance of thermodynamic correction factors on the diffusion behaviour.

4. Diffusion of binary mixtures

For diffusion of a binary mixture in silicalite Eqs. (4)–(7) reduce to

$$(N) = -\rho[D]\,\frac{\mathrm{d}(\theta)}{\mathrm{d}z},$$

$$[D] = \begin{bmatrix} \dfrac{1}{Đ_1}+\dfrac{\theta_2}{Đ_{12}} & -\dfrac{\theta_1}{Đ_{12}} \\ -\dfrac{\theta_2}{Đ_{12}} & \dfrac{1}{Đ_2}+\dfrac{\theta_1}{Đ_{12}} \end{bmatrix}^{-1} \begin{bmatrix} \Gamma_{11} & \Gamma_{12} \\ \Gamma_{21} & \Gamma_{22} \end{bmatrix}. \tag{11}$$

The interchange mechanism is often ignored and the following formulation used:

$$(N) = -\rho[D]\,\frac{\mathrm{d}(\theta)}{\mathrm{d}z},\ [D] = \begin{bmatrix} Đ_1 & 0 \\ 0 & Đ_2 \end{bmatrix} \times \begin{bmatrix} \Gamma_{11} & \Gamma_{12} \\ \Gamma_{21} & \Gamma_{22} \end{bmatrix} \text{(without interchange)}. \tag{12}$$

Recent work of Van de Graaf et al. (1999) has shown that for diffusion of binary mixtures in silicalite, the complete Maxwell–Stefan formulation, Eq. (11), taking interchange into account provides a much better description of binary permeation experimental results across a silicalite membrane than with a model ignoring the interchange mechanism (portrayed by $Đ_{12}$).

In order to calculate the Γ_{ij} we need the sorption isotherms for mixtures. However, experimental data on sorption isotherms of mixtures are extremely rare. In order to illustrate the influence of Γ_{ij} on the diffusion we consider a mixture of n-hexane (n-C_6) and 3-methyl

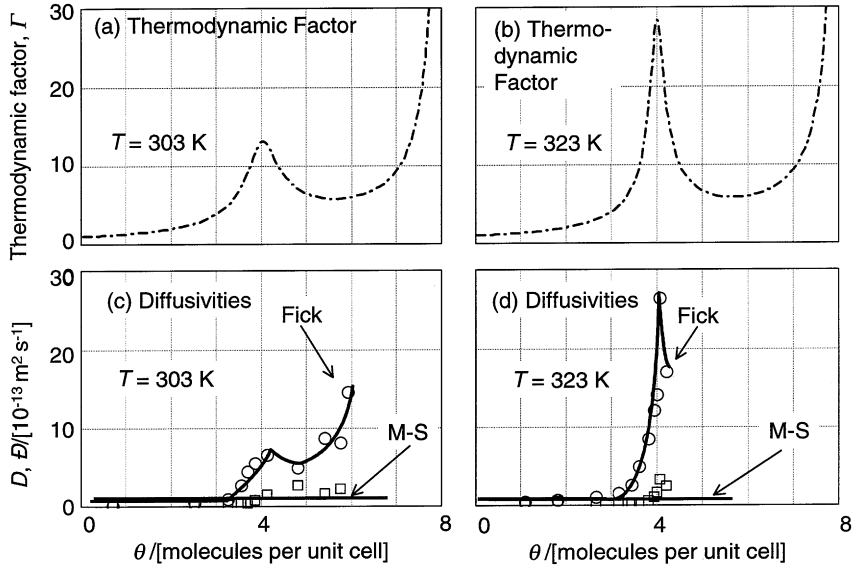

Fig. 4. Thermodynamic correction factors (a, b) and diffusivities (c, d) for diffusion of benzene in silicalite at (a, c) 303 K and (b, d) 323 K. The experimental diffusivity data are from Shah et al. (1995).

pentane (3MP) and use the CBMC simulation technique described earlier (Vlugt et al., 1998, 1999) to generate the pure component and 50–50 mixture isotherm data at 362 K. Vlugt et al. (1999) have provided extensive comparisons of CBMC simulations with experimental data on linear and branched alkanes, in the 4–9 C atom range, to demonstrate the acccuracy of the CBMC calculations. The results of these CBMC simulations are shown in Fig. 5. From the manner in which the CBMC simulations are carried out the values of the partial pressures exceeding 10^5 Pa are to be interpreted as the component fugacities. The continuous lines in Fig. 5 (a) are DSL fits of the pure component isotherms (parameter values are given in the caption). The mixture isotherms are well represented by the DSL mixture model

$$\theta_i = \frac{(\theta_A k_{iA} + \theta_B k_{iB})p_i + (\theta_A + \theta_B)k_{iA}k_{iB}p_i^2}{1 + (k_{1A} + k_{1B})p_1 + k_{1A}k_{1B}p_1^2 + (k_{2A} + k_{2B})p_2 + k_{2A}k_{2B}p_2^2}, \quad i = 1, 2 \qquad (13)$$

as can be seen in Fig. 5(b) wherein the mixture isotherms are predicted using only pure component data.

The branched alkane 3MP exhibits a curious maximum with respect to molecular loading within the silicalite structure. We see from Fig. 5 that as the partial pressures increase to 100 Pa, the sorbate loading of both linear and branched alkanes increase till a maximum is reached in the loading of 3MP. This occurs at a total loading of 4 molecules per unit cell. Up to this point there is really no competition between n-C_6 and 3MP and both are almost equally easily adsorbed. Examination of the probability distributions of the linear and branched isomers at 100 Pa shows that all the 3MP molecules are located at the intersections between the straight channels and the zigzag channels (Fig. 6) whereas n-C_6 are located everywhere; a schematic is shown in Fig. 6. The n-C_6 molecules fit nicely into both straight and zigzag channels (Smit and Maesen, 1995); these molecules have a higher 'packing efficiency' than 3MP. As the pressure is increased beyond 100 Pa, it is more efficient to obtain higher loading by 'replacing' the 3MP with n-C_6; this entropic effect is the reason behind the curious maximum in the 3MP isotherm. The same phenomena has been observed earlier for hydrocarbon mixtures of linear and 2-methyl alkanes with 4–7 C atoms (Krishna et al., 1998).

The four elements of Γ_{ij} can be obtained by analytic differentiation of Eq. (13). The results are

$$[\Gamma] \equiv \frac{\begin{bmatrix} A_3(B_2 - \theta_2 B_4)/p_1 & A_3\theta_1 B_4/p_1 \\ B_3\theta_2 A_4/p_2 & B_3(A_2 - \theta_1 A_4)/p_2 \end{bmatrix}}{A_2B_2 - \theta_1 A_4 B_2 - \theta_2 A_2 B_4}, \qquad (14)$$

where

$$A_2 = (\theta_{1A}k_{1A} + \theta_{1B}k_{1B}) + (\theta_{A1} + \theta_{B1})k_{1A}k_{1B}(2p_1),$$
$$A_3 = (\theta_{1A}k_{1A} + \theta_{1B}k_{1B})p_1 + (\theta_{A1} + \theta_{B1})k_{1A}k_{1B}p_1^2,$$
$$A_4 = (k_{1A} + k_{1B}) + k_{1A}k_{1B}(2p_1),$$
$$B_2 = (\theta_{2A}k_{2A} + \theta_{2B}k_{2B}) + (\theta_{2A} + \theta_{2B})k_{2A}k_{2B}(2p_2),$$

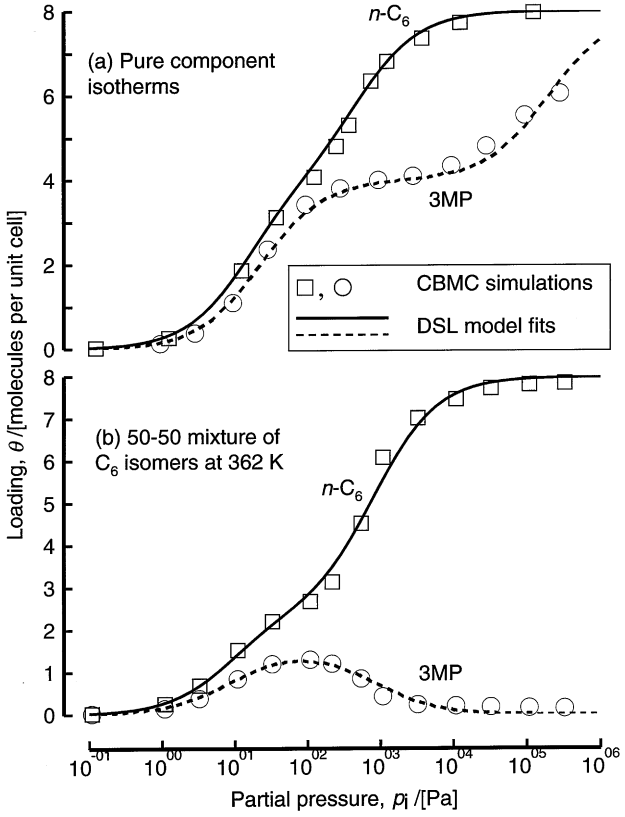

Fig. 5. Pure component and 50–50 mixture isotherms at 362 K in silicalite. The open square and circle symbols represent the CBMC simulations for (1) n-C_6 and (2) 3MP, respectively. The continuous and dashed lines are the dual-site Langmuir (DSL) fits with the parameter values determined only from pure component CBMC simulation data. The dual-site Langmuir parameter values are for n-C_6: $\theta_{1A} = 4$, $\theta_{1B} = 4$, $k_{1A} = 0.07\ \mathrm{Pa}^{-1}$, $k_{1B} = 2 \times 10^{-3}\ \mathrm{Pa}^{-1}$ and for 3MP: $\theta_{2A} = 4$, $\theta_{2B} = 4$, $k_{2A} = 0.045$, $k_{2B} = 5 \times 10^{-6}$.

$$B_3 = (\theta_{2A}k_{2A} + \theta_{2B}k_{2B})p_2 + (\theta_{2A} + \theta_{2B})k_{2A}k_{2B}p_2^2,$$

$$B_4 = (k_{2A} + k_{2B}) + k_{2A}k_{2B}(2p_2). \qquad (15)$$

To demonstrate the consequences of the influence of Γ_{ij} on diffusion, consider the permeation of hydrocarbon isomers across a silicalite membrane (Fig. 7). In order to obtain the values of the permeation fluxes N_i we need to solve the set of two coupled partial differential equations:

$$\frac{\partial(\theta)}{\partial t} = \frac{\partial}{\partial z}\left([D]\frac{\partial(\theta)}{\partial z}\right) \qquad (16)$$

subject to the initial and boundary conditions

$$t = 0,\ 0 \leqslant z \leqslant \delta,\ \theta_{iz} = 0, \qquad (17a)$$

$$t \geqslant 0,\ z = 0,$$

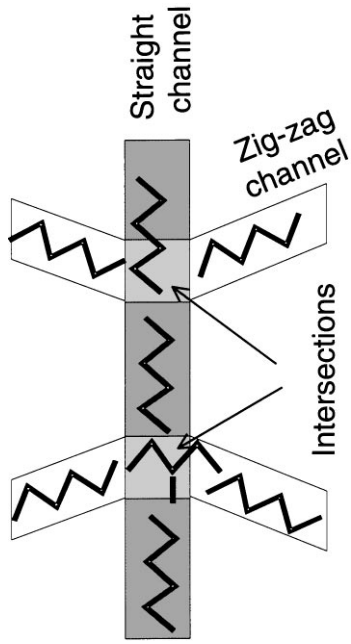

Fig. 6. Preferential siting of 3 MP alkanes at the intersections between the straight and zig-zag channels. The linear alkane can be located at any position within the silicalite structure.

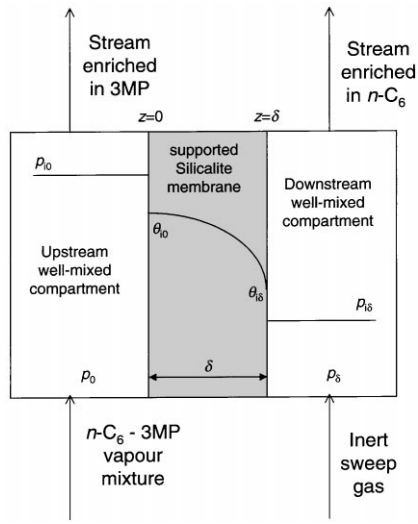

Fig. 7. Schematic of silicalite membrane separation process for separation of C_6 isomers.

The set of two coupled partial differential equations (16) subject to the initial and boundary conditions (17) were solved using the method of lines (Schiesser, 1991) to determine the fluxes, as described in our earlier work (Krishna and Van den Broeke, 1995). In the calculations

$$\theta_{i0} = \frac{(\theta_A k_{iA} + \theta_B k_{iB})p_{i0} + (\theta_A + \theta_B)k_{iA}k_{iB}p_{i0}^2}{1 + (k_{1A} + k_{1B})p_{10} + k_{1A}k_{1B}p_{10}^2 + (k_{2A} + k_{2B})p_{20} + k_{2A}k_{2B}p_{20}^2}, \quad i = 1, 2. \qquad (17b)$$

presented in this paper we assume that the pure component Maxwell–Stefan diffusivities are identical for the isomers, i.e. $Đ_{1Z} = Đ_{2Z}$; this assumption is a conservative one from the viewpoint of separation of the isomers as we expect the branched isomer to have a lower mobility within the silicalite structure. The simulations were carried out with the complete Maxwell–Stefan model for $[Đ]$, i.e. Eq. (11). Since the interchange coefficient $Đ_{12}$ has a value intermediate between $Đ_{1Z}$ and $Đ_{2Z}$ (Krishna, 1990) we must also have $Đ_{1Z} = Đ_{2Z} = Đ_{12}$. A further point to note is that in the calculation of the fluxes we have made the assumption that the Maxwell–Stefan diffusivities are independent of the loading. Though this assumption is not always true (see e.g. Krishna and Weselingh, 1997), the values of the ratio of fluxes, i.e. selectivity for separation, is not expected to be influenced by this assumption.

The transient fluxes for the C_6 isomers are presented in Fig. 8 in dimensionless form. Examination of the transient fluxes reveals a slight maximum in the flux of the branched alkanes; this maximum is a direct consequence of the corresponding maximum in mixture isotherms; see Fig. 5(b). The ratio of the fluxes of *n*-C_6 and 3MP is found to be 32. There is some evidence in the published literature for permeation of a 50–50 mixture of *n*-C_6 and 3MP at 362 K across a silicalite membrane (Funke et al., 1997) to suggest that this high selectivity values for separation of the C_6 isomers can be realised in practice. These high selectivities are entirely due to the strong inflection observed for the branched alkane; this is described by a much lower value of the Henry coefficient k_B for site B than for the linear alkane. If both sites A and B had the same sorption capability, then the selectivity for the separation would be close to unity. Another important point to note is that in the membrane permeation experiment we must ensure that the values of the upstream partial pressures of the hydrocarbon isomers are high enough (say higher than 5 kPa) to ensure that the branched alkane is virtually 'excluded'.

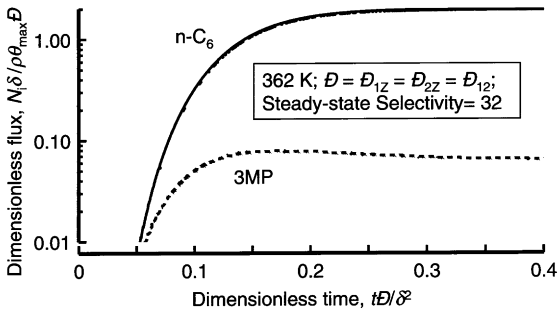

Fig. 8. Transient diffusion fluxes for permeation of *n*-C_6 and 3MP across a silicalite membrane. The conditions used in the simulations are identical to those used in the experiments of Funke et al. (1997). The upstream and downstream compartments are maintained at a total pressure of 84 kPa (atmospheric pressure at Boulder, Colorado, USA). In the upstream compartment the hydrocarbons account for 18 mol%, the remainder being inert gas helium. The partial pressures of *n*-C_6 and 3MP in the upstream compartment work out to 0.18×42 kPa for each isomer. An excess of sweep gas in the downstream compartment ensures that the partial pressures of the hydrocarbons are virtually zero.

5. Conclusions

Isotherm inflection behaviour can be modeled using the dual-site Langmuir model. The consequences of the isotherm inflection on the diffusion characteristics have been examined with the help of the Maxwell–Stefan diffusion equations. For single component diffusion in silicalite, the Fick diffusivity can exhibit two extrema.

For a binary mixture consisting of *n*-C_6 and 3MP, the DSL model anticipates a curious maximum in the loading of the branched alkane in conformity with CBMC simulations. The Maxwell–Stefan theory for binary diffusion is used to demonstrate the possibility of separating hydrocarbon isomers by relying on diffusion selectivity across a silicalite membrane.

Notation

A_2, A_3, A_4	parameters defined in Eq. (15)
B_2, B_3, B_4	parameters defined in Eq. (15)
$[Đ]$	matrix of Fick diffusivities, m^2/s
$Đ_{iZ}$	Maxwell–Stefan diffusivity for species-zeolite interchange, m^2/s
$Đ_{ij}$	Maxwell–Stefan diffusivity describing interchange between i and j, m^2/s
k_A	Henry coefficient for site A, Pa^{-1}
k_B	Henry coefficient for site B, Pa^{-1}
n	number of species in mixture, dimensionless
N_i	molecular flux of species i, molecules/m^2/s
p_i	partial pressure of species i, Pa
R	gas constant, 8.314 J/mol/K
t	time, s
T	absolute temperature, K
z	direction coordinate, m

Greek letters

δ	thickness of membrane, m
Γ	thermodynamic correction factor, dimensionless
$[\Gamma]$	matrix of thermodynamic correction factors, dimensionless
Γ_{ij}	elements of matrix of thermodynamic correction factor, $[\Gamma]$, dimensionless
μ	chemical potential, J/mol
θ	loading, molecules per unit cell
θ_A	maximum loading of site A
θ_B	maximum loading of site B

θ_{max} maximum loading in the zeolite, $\theta_{max} = (\theta_A + \theta_B)$
η dimensionless distance along membrane, dimensionless
ρ density of membrane, number of unit cells per m^3

Subscripts

A referring to site A, intersections
B referring to site B, channel interiors
1 component 1 in binary mixture
2 component 2 in binary mixture
max referring to maximum loading
Z referring to zeolite

References

Funke, H.H., Argo, A.M., Falconer, J.L., & Noble, R.M. (1997). Separation of cyclic, branched, and linear hydrocarbon mixtures through silicalite membranes. *Ind. Engng Chem. Res.*, *36*, 137–143.

Guo, C.J., Talu, O., & Hayhurst, D.T. (1989). Phase transition and structural heterogeneity: Benzene adsorption on silicalite. *A.I.Ch.E. J.*, *35*, 573–578.

Krishna, R. (1990). Multicomponent surface diffusion of adsorbed species. A description based on the generalized Maxwell–Stefan diffusion equations. *Chem. Engng Sci.*, *45*, 1779–1791.

Krishna, R. (1993a). Problems and pitfalls in the use of the Fick formulation for intraparticle diffusion. *Chem. Engng Sci.*, *48*, 845–861.

Krishna, R. (1993b). A unified approach to the modelling of intraparticle diffusion in adsorption processes. *Gas Separation and Purification*, *7*, 91–104.

Krishna, R., & van den Broeke, L.J.P. (1995). The Maxwell–Stefan description of mass transport across zeolite membranes. *Chem. Engng J.*, *57*, 155–162.

Krishna, R., & Wesselingh, J.A. (1997). The Maxwell–Stefan approach to mass transfer. *Chem. Engng Sci.*, *52*, 861–911.

Krishna, R., Smit, B., & Vlugt, T.J.H. (1998). Sorption-induced diffusion–selective separation of hydrocarbon isomers using silicalite. *J. Phys. Chem. A*, *102*, 7727–7730.

Micke, A., Bülow, M, Kocirik, M., & Struve, P. (1994). Sorbate immobilization in molecular sieves. Rate-limiting step for *n*-hexane uptake by silicalite-1. *J. Phys. Chem.*, *98*, 12,337–12,344.

Ruthven, D.M. (1984). *Principles of adsorption and adsorption processes.* (p. 91). New York: Wiley.

Schiesser, W.E. (1991). *The numerical method of lines: Integration of partial differential equations.* San Diego: Academic Press.

Shah, D.B., Guo, C.J., & Hayhurst, D.T. (1995). Intracrystalline diffusion of benzene in silicalite: Effect of structural heterogeneity. *J. Chem. Soc. Farad. Trans.*, *91*, 1143–1146.

Smit, B., & Maesen, T.L.M. (1995). Commensurate 'freezing' of alkanes in the channels of a zeolite. *Nature*, *374*, 42–44.

Song, L., & Rees, L.V.C. (1997). Adsorption and transport of n-hexane in silicalite-1 by the frequency response technique. *J. Chem. Soc. Farad. Trans.*, *93*, 649–657.

Sun, M.S., Talu, O., & Shah, D.B. (1996). Adsorption equilibria of C_5–C_{10} normal alkanes in silicalite crystals. *J. Phys. Chem.*, *100*, 17,276–17,280.

Sun, M.S., Shah, D.B., Xu, H.H., & Talu, O. (1998). Adsorption equilibria of C_1–C_4 alkanes, CO_2 and SF_6 on silicalite. *J. Phys. Chem.*, *102*, 1466–1473.

Takaishi, T., Tsutsumi, K., Chubachi, K., & Matsumoto, A. (1998). Adsorption induced phase transition of ZSM-5 by *p*-xylene. *J. Chem. Soc. Farad. Trans.*, *94*, 601–608.

Van de Graaf, J., Kapteijn, F., & Moulijn, J.A. (1998). Methodological and operational aspects of permeation measurements on silicalite-1 membranes. *J. Memb. Sci.*, *144,* 87–104.

Van de Graaf, J., Kapteijn, F., & Moulijn, J.A. (1999). Modeling permeation of binary mixtures through zeolite membranes. *A.I.Ch.E. J.* (in press).

Vlugt, T.J.H., Zhu, W., Kapteijn, F., Moulijn, J.A., Smit B., & Krishna, R. (1998). Adsorption of linear and branched alkanes in the zeolite silicalite-1. *J. Am. Chem. Soc.*, *120*, 5599–5600.

Vlugt, T.J.H., Krishna, R., & Smit, B. (1999). Molecular simulations of adsorption isotherms of linear and branched alkanes and their mixtures in silicalite. *J. Phys. Chem. B*, *103*, 1102–1118.